RSC Advances

ROYAL SOCIETY OF CHEMISTRY

www.rsc.org/advances

Ultrafast Dynamics of a Molecular Rotor in Chemical and Biological Nano-Cavities

Krishna Gavvala, Sagar Satpathi, Partha Hazra*

Department of Chemistry, Indian Institute of Science Education and Research (IISER), Pune 411008, Maharashtra, India.

* Corresponding author. E-mail: p.hazra@iiserpune.ac.in. Tel.: +91-20-2590-8077; Fax: +91-20-2589 9790.

Abstract

Molecular rotors have become indispensable tools to monitor several important processes in chemistry and biology owing to their sensitivity towards viscosity. Despite their importance, less attention has been paid to understand the excited state properties of molecular rotors. Recently, Maroncelli and coworkers unraveled the excited state photochemistry of julolidine based molecular rotor, 9-(2-carboxy-2-cyano)vinyl julolidine (CCVJ), and claimed that CCVJ is not a simple rotor probe. Unlike other molecular rotors, the photoisomerization is believed to be the main non-radiative decay pathway for this molecule. Inspired by their report, herein, we have tried to understand how the excited state dynamics of CCVJ is getting affected inside the nano-cavities of cyclodextrins (CDs) and human serum albumin (HSA) protein using steady-state and femtosecond fluorescence up-conversion techniques. We have observed pronounced enhancement in fluorescence quantum yield, when CCVJ is encapsulated in CDs (β- and γ-CD) and HSA. Femtosecond up-conversion study reveals that the ultrafast dynamics of CCVJ is drastically retarded inside the nano-cavities of CDs and protein. All these results suggest that photoisomerization, which is believed to be major non-radiative decay pathway of CCVJ, is severely restricted inside the above mentioned bio-mimetic and biological nano-cavities. The molecular pictures of orientations of CCVJ inside the nano-cavities of CDs and protein have been discussed by theoretical and molecular modeling studies. We believe the present results might be helpful in exploiting this molecule more in biological and viscosity sensing applications.

Keywords: molecular rotor, CCVJ, cyclodextrin, HSA, fluorescence upconversion.

Introduction

Molecular rotors, a special class of fluorescent molecules, are used to probe many important chemical and biological processes, like polymerization progress, peptide-protein interaction, assembly processes of tubulin, phase transition of phospholipid bilayers.[1-6] They have also been employed to probe local viscosity in simple, complex and biological media.[7-15] Among various molecular rotors, 9-(dicyanovinyl)-julolidine (DCVJ) and 9-(2-carboxy-2-cyano)vinyl-julolidine (CCVJ) are the most commonly used molecular rotors. Different mechanisms have been proposed regarding the excited state process responsible for the environmental sensitivity of these probes. Computational and experimental studies suggested isomerization about the double bond (similar to the well-known behavior of styryl compounds[16]) is mainly accountable for the excited state non-radiative decay pathway of these types of molecules.[17] The TICT mechanism, which involves the twisting of aryl-alkenyl single bond, is also still widely accepted non-radiative decay channels of these types of molecules.[13, 18-20] In order to address this issue, very recently, Marconcelli and co-workers explored the excited state photochemistry of CCVJ.[21] They reported the isomerization, rather than the commonly assumed TICT process, that dictates viscosity-sensing ability of CCVJ. In hydroxylic solvents, CCVJ exists primarily in the carboxylate form of E isomer (Scheme 1).[21] Apart from the above mentioned studies limited study on this molecule is devoted to understand its excited state dynamics. In the present work, we have taken an attempt to understand how the non-radiative decay pathways including photo-isomerization process would be affected in confined environments. Moreover, in order to exploit this molecule in biological applications, it is necessary to have a proper knowledge about the environment-dependent fluorescence properties of CCVJ, which is lacking in literature. In an endeavor to address the aforesaid points, we have investigated the excited state fluorescence properties

inside bio-mimicking nanocavities, i.e., cyclodextrins (CDs), as model supramolecular nano-cavities and protein nano-cavity, i.e, human serum albumin (HSA) as a model protein.

Herein, for the first time, we have explored the ultrafast dynamics of CCVJ in aqueous solution, CDs and HSA using femtosecond fluorescence up-conversion technique. Excited state dynamics of CCVJ is found to be strongly dependent on surrounding confinement effect of the medium. Importantly, fluorescence quantum yield of CCVJ is enhanced many folds in CDs and protein due to the retardation of non-radiative processes inside the nano-cavities of hosts and HSA. Fluorescence lifetime of CCVJ becomes several times slower inside the nano-cavities of CDs and HSA, confirming the restriction of rotational motions of CCVJ inside the above mentioned constrained media. Finally, the possible orientations of CCVJ inside the nano-cavities of CDs and protein have been anticipated by molecular modeling and theoretical studies.

Materials and methods

CCVJ (purity ≥97%, HPLC), CDs and HSA were purchased from Sigma Aldrich, and used without further purification. All the experiments were done in 10 mM sodium phosphate buffer of pH 7. CD/HSA was gradually added to the solution containing CCVJ, and the solution was gently shaken after each addition until CD was completely solubilized.

Absorption measurements were performed on Perkin-Elmer UV-visible spectrophotometer (Lambda-45), and steady-state fluorescence spectra were recorded with Fluoromax-4 spectrofluorometer (Horiba Jobin Yvon). Time-resolved fluorescence measurements were initially collected on time correlated single photon counting (TCSPC) spectrometer (Horiba Jobin Yvon IBH, U.K.). The detail description of the instrument is described elsewhere.[22] Briefly, in the present work a 440 nm diode laser (~100 ps, 1 MHz repetition rate) was used as the excitation source and MCP-PMT detector was used for

collecting fluorescence signal. The analysis of the lifetime was done by IBH DAS6 analysis software.

Ultrafast fluorescence decay transients were measured using femtosecond fluorescence up-conversion setup (FOG 100, CDP) whose description was given elsewhere.[23] Briefly, the sample was excited at 420 nm using the second harmonic of a mode-locked Ti-sapphire laser (Mai-Tai, Spectra Physics). The fluorescence emitted from the sample was up-converted in another nonlinear crystal using a gate pulse (840 nm) of the fundamental beam. The sum frequency of the fluorescence and gate pulse was detected as a function of the time delay between excitation and gate pulses. The angle between the polarization of the pump and gate pulses was kept at the magic angle to eliminate effects from rotational diffusion. The up-converted signal was dispersed in a monochromator and detected using photon counting electronics. A cross-correlation function obtained using the Raman scattering from ethanol provided a full-width at half-maximum (fwhm) of ~350 fs. Estimated uncertainties in the up-conversion measurements are ~15-20%.

Molecular docking was done by the standard protocol and the details are described elsewhere.[24] CD was taken as receptor and the anion form of CCVJ, i.e, E isomer was taken as ligand in the docking protocol. During docking the receptor was kept rigid and the ligand was flexible. In all docking we have used Gasteiger charges for both the CDs and the ligand. The grid was generated on a whole receptor with grid points of 60 on each of the orthogonal directions with a spacing of 0.16 Å. Search was performed using Genetic algorithm. Finally, all the docked complexes were fully optimized by PM3 semi-empirical methods using Gaussian software.[25]

Results and discussion

Steady-state results:

CCVJ exhibits absorption maximum at 430 nm in aqueous buffer solution (Figure 1**)**. In presence of CDs, the absorption profiles exhibit some changes depending upon the cavity sizes of CDs. As shown in Figure 1a, no change is observed in absorption spectra in presence of α-CD, suggesting no significant interactions between CCVJ and α-CD. Unlike α-CD case, the absorption maximum of CCVJ undergoes hypsochromic shift in presence of β-CD (Figure 1b), and this observation infers that there exists a considerable interaction between CCVJ and β-CD. In presence of γ-CD, analogous results are observed indicating similar kinds of interactions are present in both of these host molecules. The hypsochromic shift in absorption profiles in presence of CDs (β- and γ-CD) is indicative towards the change in polarity of CCVJ surroundings when it interacts with β- and γ-CD. In summary, the absorption results infer that ground state of CCVJ molecule interacts with β and γ-CD.

To get insight into the excited state properties, emission profiles of CCVJ are monitored in absence and presence of various cavity sized CDs. CCVJ exhibits weak fluorescence (Φ_f = 0.0016)[11] with emission maximum situated at 500 nm in neutral buffer solution **(**Figure 2**)**. Here it is pertinent to mention that CCVJ exists mainly in carboxylate form (E isomer) in buffer or water. However, when E isomers are excited, they convert to non-fluorescent Z isomer. Hence, the observed fluorescence spectrum with a peak ~500 nm is originated from the S_1 state of E isomers of CCVJ. In presence of α-CD, slight increment in fluorescence quantum yield is found (~1.3 times) without showing any hypsochromic shift (Figure 2a, Table 1). However, a significant alteration in emission profiles is observed in presence of β-CD. Here, a ~10 fold enhancement in fluorescence quantum yield is noticed (Figure 2b, Table 1) at highest concentration of β-CD. Besides the increment in quantum yield, a hypsochromic shift from 500 nm to 475 nm is observed. The above findings infer the

strong interaction between CCVJ and β-CD, whereas weak interaction may prevail with α-CD. The observed hypsochromic peak shift suggests that E isomers are in less polar environment in presence of β-CD, as it is reported that E isomer is sensitive to the polarity of the surrounding environment[21]. This confirms that E isomers are displaced from water environment, and subsequently, they are getting encapsulated inside the less polar nano-cavity of β-CD. The increment in fluorescence quantum yield can be ascribed to the inhibition of photoisomerization process, which is believed to the main non-radiative decay pathways of CCVJ[21]. As there is no hypsochromic shift observed in case of α-CD, the possibility of inclusion complex formation between α-CD and CCVJ can be ruled out. This is further justified considering the cavity size of CD (the internal cavity diameter of α-CD is 5.7 Å) and size of CCVJ molecule (according to the geometry optimized structure, the width of a CCVJ molecule is ~7 Å along the julolidine group and the length of a CCVJ molecule is ~9.2 Å). However, partial inclusion complex (incorporation of cyano, carboxy-vinyl group of CCVJ) as well as hydrogen bond interaction between carboxyl group and -OH groups of α-CD cannot be ruled out at this moment. To confirm the latter possibility, we have performed a control experiment with glucose. But no significant enhancement in fluorescence intensity is observed (Figure S1) confirming hydrogen bond interaction between carboxyl/cyano group of CCVJ and -OH groups is not responsible for the observed change in presence of α-CD. Similar to β-CD, the fluorescence quantum yield of CCVJ increases continuously with gradual addition of γ-CD (Figure 2c, Table 1), and at maximum γ-CD concentration, ~4.5 fold increment in fluorescence quantum yield along with 10 nm hypsochromic shift is observed. Certainly, this increment as well as shift is less compared to β-CD. The dissimilar extent of rise in quantum yield in CDs is due to the different extent of rigidity felt by E isomers of CCVJ in various CDs. Therefore, cavity size of host has a major role in the observed changes in fluorescence quantum yield of CCVJ in different CD. Among all three

CDs, the increment in fluorescence quantum yield of CCVJ is more in case of β-CD, and it is attributed to the more restricted environment inside β-CD nano-cavity. Since the internal cavity diameter of β-CD is ~7 Å and depth of the cavity is ~8 Å, CCVJ molecule can perfectly fit inside the nano-cavity of β-CD, thereby, restricting its rotational motion along the vinyl bond as well as twisting motion along aryl-alkenyl single bond. On the other hand, the internal cavity diameter of γ-CD (~9 Å) is large enough compared to the size of E isomer. As a result, the incorporation of CCVJ molecule into the γ-CD cavity cannot fully restrict the photo-isomerisation process, which is believed to be main non-radiative decay pathway of CCVJ molecule[21]. The large hypsochromic shift inside the β-CD cavity is attributed to the less polar nano-cavity experienced by the E isomer of CCVJ compared to γ-CD nano-cavity. To gain more insight into the inclusion complex formation, stoichiometry and association constants are calculated using Benesi-Hildebrand (BH) equation.[26]

$$\frac{1}{F - F_0} = \frac{1}{K_a(F_1 - F_0)[CD]} + \frac{1}{F_1 - F_0} \qquad (1)$$

where F_0, F and F_1 are the fluorescence intensities of E isomer of CCVJ in absence, presence of host, and in the inclusion complex, respectively. The double reciprocal plot of 1/ΔF vs 1/[CD] yields a straight line (Figure S2), confirming 1:1 stoichiometry for both β- and γ-CD. The association constants for β- and γ-CD are calculated to be ~1300 (±100) M^{-1} and 450 (±20) M^{-1}, respectively. The three times higher binding constant for β-CD is in good agreement with our conjecture that CCVJ forms more stable inclusion complex with β-CD than γ-CD.

Time-resolved fluorescence study:

Since the internal molecular rotations of CCVJ are expected to be severely restricted on forming inclusion complex with CDs, it is expected that fluorescence lifetime of CCVJ

should be affected inside the nano-cavities of CDs. Therefore, we have probed the inclusion complex formation by monitoring the fluorescence lifetime of CCVJ in presence of CDs. In buffer solution, CCVJ exhibits fast decay comparable with the time-response of our TCSPC set-up, i.e., IRF. Hence, it cannot be resolved using TCSPC set-up (Figure S3). Thus, we have used the fluorescence up-conversion technique to unravel the ultrafast dynamics of CCVJ (Figure 3). In buffer solution, the emission decay of CCVJ is well represented as mono-exponential function with a lifetime of ~2.87 ps (Table 1). Notably, this is the first ever report regarding the excited state lifetime of CCVJ in water environment. As the E isomer of CCVJ is only emissive in nature, the detected lifetime certainly reflects the excited state lifetime of E isomer in water environment. Short lifetime (~2.87 ps) observed in water indicates that non-radiative decay pathway mainly via photoisomerization process[21] reduce its excited state lifetime. In presence of α-CD, the decay fits well with two lifetime components of 2.90 ps (90%) and 16 ps (10%) (Figure 3, Table 1). The fast lifetime component is attributed to the un-complexed CCVJ in solution, whereas the longer lifetime component (16 ps) may appear as a result of interaction between CCVJ and α-CD. The smaller amplitude of long component indicates that minute populations of E isomers are interacting with the host. As the molecule cannot be accommodated inside the cavity of α-CD (confirmed from steady state results), hence, the observed 16 ps lifetime may be attributed to some sort of partial inclusion complex formation, which slightly suppresses the photoisomerization process, which is believed to be main non-radiative decay pathway for CCVJ[21]. More evidences for the partial inclusion complex formation are provided by the docking and computational studies given later part of the manuscript. In presence of β- and γ-CD, the decay profiles of CCVJ also exhibit bi-exponential in nature. In both the cases, long lifetime component (35 ps and 24 ps, for β and γ-CD, respectively) along with fast component (originated from the uncomplexed CCVJ molecules) is detected (Figure 3, Table 1). The large increment in

lifetime values can be explained in terms of restriction of photoisomerization process around the vinyl bond (which is believed to be main non-radiative decay pathway of CCVJ) in the inclusion complexes. As a result, the non-radiative decay pathways are significantly reduced. The longer lifetime of CCVJ in case of β-CD is attributed to the formation of more rigid complex with β-CD than γ-CD due to perfect fitting of CCVJ inside the β-CD cavity, whereas γ-CD having bigger cavity size may not hold the CCVJ molecule as tightly as that of β-CD cavity.

To get more insights about radiative and non-radiative decay pathways, we have calculated radiative (k_r) and non-radiative (k_{nr}) decay rate constants by the following equations:

$$\Phi_f = \frac{k_r}{k_r + \Sigma k_{nr}} \qquad (2)$$

$$\tau_f = \frac{1}{k_r + \Sigma k_{nr}} \qquad (3)$$

The calculated decay rate constants (considering lifetime component of bound CCVJ) are summarized in Table 1. Here it is pertinent to mention that the long lifetime components, which reflect the lifetime of bound CCVJ, are considered for calculating k_r and k_{nr}. The very low k_r and high k_{nr} values are in good agreement with very low fluorescence quantum yield as well as faster lifetime component of CCVJ in water. In presence of α-CD, the k_r value increases ~3.5 times; however, k_{nr} value decreases almost 5.5 times. Considering steady state and lifetime results, the increment in k_r and decrement in k_{nr} values may be attributed to the formation of partial inclusion complex between CCVJ and α-CD. In presence of β-CD, almost 14 times decrement in k_{nr} value confirms that the non-radiative internal rotations are drastically reduced inside the nano-cavity of supramolecular host. For γ-CD, almost similar observations are found. However, in this case, suppression of k_{nr} value is less (~8.75 times) as

compared to β-CD. The lower k_{nr} value inside the β-CD nano-cavity can be attributed to the formation of more rigid inclusion complex with E isomer, hence the restriction of internal molecular rotations (mainly includes photoisomerization process[21]) is more. In summary, lifetime results and decay rate constants are in good agreement with steady state findings.

Binding interactions with HSA:

It is not enough to examine the dynamics of CCVJ inside bio-mimicking chemical nano-cavities, but it is also necessary to understand the effect of confinement of biological medium on excited state properties of CCVJ. Therefore, we have investigated the environment-dependent fluorescence of CCVJ inside a model protein (HSA) in the context of specific biomolecular interactions. Absorption and emission spectra of CCVJ in absence and presence of HSA are shown in Figure 4. Absorption maximum of CCVJ undergoes blue shift in presence of HSA. In emission spectra, a huge enhancement in quantum yield (~55 times) accompanied by hypsochromic shift is observed with gradual addition of HSA. The vast increment in fluorescence quantum yield confirms the strong binding affinity of CCVJ with protein, whereas the blue shift in emission peak is attributed to reduced polarity experience by E isomers of CCVJ inside the protein binding pocket. The results bear a close resemblance to the observations with CDs (β-CD and γ-CD). However, the huge increment in quantum yield and blue shift (Figure 4), indicating the strong binding affinity of E isomers towards HSA. Binding constant (K_a) with HSA is calculated by using equation 1. The association constant (K_a) is found to be 1.0×10^5 M^{-1} (Figure S4**)**. Certainly, this value is several folds higher than the binding constant observed in presence of β-CD inferring that CCVJ binds strongly to HSA than that of β-CD.

To gain deeper insight into the underlying photo-physical behaviour of the rotor upon interaction with protein, fluorescence lifetime measurements were performed for CCVJ in presence of protein environment. The fluorescence up-converted decay profile of CCVJ in

presence of HSA exhibits comparably slow lifetime (~84 ps) component (Figure 3). This time constant is certainly higher than CCVJ:β-CD complex, where ~35 ps lifetime component is observed. Moreover, a 30 times decrease in k_{nr} value compared to uncomplexed CCVJ is observed. Lower k_{nr} and longer lifetime value compared to CDs confirms that the inhibitions of non-radiative internal molecular rotations are more inside the protein nano-cavity. As the E to Z conversion is one of the major non-radiative decay pathways[21], we believe that this conversion process is getting restricted more inside the protein nano-cavity as compared to cyclodextrin nano-cavities.

Molecular docking and computational study:

To obtain molecular picture of orientation of CCVJ in the inclusion complexes, we have docked the ligand into CDs, followed by quantum chemical calculations. The optimized structures are shown in Figure 5. As shown in the Figure 5, CCVJ is encapsulated inside the CDs (β- and γ-CD) in such a way that both vinyl bond (having cyano and carboxylate groups) as well as aryl-alkenyl single bond stay inside the nano-cavities, thereby, twisting and/or conversion of E to Z isomers are believed to be reduced drastically inside the nano-cavity. Whereas in case of α-CD, the CCVJ is not completely encapsulated in the nano-cavity, instead it resides at the hydroxyl portals of the CD with cyano and carbaxylate groups projected partially towards the cavity. This partial encapsulation of CCVJ results in the slight restriction of internal molecular rotation, which is believed to be responsible for the observed changes in steady state and time resolved results. The smaller cavity size of β-CD compared to γ-CD might be responsible for the observed vivid changes in presence of β-CD. In a nutshell, the computational studies further support and confirm the experimental evidences.

To locate the dye in protein nano-cavity, the CCVJ is docked with HSA. Here negatively charged E isomer of CCVJ is taken as ligand because it exists as anion in solution. Figure 6 shows CCVJ docked protein complex with minimum energy in the cluster analysis.

The most stable or least energetic structure clearly depicts that CCVJ resides at domain II (IIA) binding pocket of protein. This binding site is well-known to have higher binding affinities for negatively charged ligands,[27-30] and, therefore the location of CCVJ in this binding pocket is justified. The less polarity at this binding site is believed to be responsible for observed blue shift in steady state emission spectrum.[27-30] Moreover, the negatively charged E isomer of CCVJ is surrounded by positively charged basic amino acid residues Lys286, Arg257, Lys289 and His242. These basic amino acids may be the main driving force for grabbing CCVJ towards the binding pocket IIA of protein. Particularly, carboxy and cyano groups of CCVJ are involved in hydrogen bond interactions with two basic amino acids (Lys199 and Arg222). Therefore, the E isomer of CCVJ is believed to be stabilized by positively charged amino acids located at this binding site through both electrostatic and hydrogen bonding interactions (Figure 6b).

Conclusion

Here, we have investigated the excited state dynamics of CCVJ in presence of molecular containers (cyclodextrins (CDs)) and protein (human serum albumin (HSA)) environments. The marked enhancement in fluorescence quantum yield as well as hypsochromic shift indicates that CCVJ molecules are displaced from water and being encapsulated inside the less polar nano-cavities of CDs (β- and γ-CD) and HSA, whereas partial inclusion complex formation is observed for α-CD. Femtosecond fluorescence up-conversion study reveals the ultrafast dynamics of CCVJ is severely hindered inside the nano-cavities of CDs and protein due to the restriction imposed on free internal molecular rotation of CCVJ. As a result, fluorescence lifetime significantly increases inside the above mentioned constrained media. Interestingly, in accordance with quantum yield and lifetime results, the non-radiative rate constants decrease several times inside the above mentioned nano-cavities. However, the

extent of decrement depends on the cavity size. All the above observations lead us to conclude that photo-isomerization process, which is believed to be major non-radiative decay pathway of CCVJ, is severely restricted inside the above mentioned bio-mimetic and biological nano-cavities. The possible orientations of CCVJ inside the nano-cavities of CDs and protein have been discussed by theoretical and molecular modeling studies.

Acknowledgement

Authors thank IISER-Pune for providing excellent experimental and computation facilities. Authors are thankful to anonymous reviewers for their valuable comments and suggestions.

References

1. K. Y. Law and R. O. Loutfy, *Macromolecules*, 1981, **14**, 587-591.
2. R. O. Loutfy, *Macromolecules*, 1983, **16**, 678-680.
3. W. L. Goh, M. Y. Lee, T. L. Joseph, S. T. Quah, C. J. Brown, C. Verma, S. Brenner, F. J. Ghadessy and Y. N. Teo, *J. Am. Chem. Soc.*, 2014, **136**, 6159-6162.
4. C. E. Kung and J. K. Reed, *Biochemistry*, 1989, **28**, 6678-6686.
5. S. Luka, *J. Am. Chem. Soc.*, 1984, **106**, 4386-4392.
6. M. Lindgren, K. Sörgjerd and P. Hammarström, *Biophys. J.*, 2005, **88**, 4200-4212.
7. H. Jin, M. Liang, S. Arzhantsev, X. Li and M. Maroncelli, *J. Phys. Chem. B*, 2010, **114**, 7565-7578.
8. J. A. Levitt, P.-H. Chung, M. K. Kuimova, G. Yahioglu, Y. Wang, J. Qu and K. Suhling, *ChemPhysChem*, 2011, **12**, 662-672.
9. H. Jin, X. Li and M. Maroncelli, *J. Phys. Chem. B*, 2007, **111**, 13473-13478.
10. A. Paul and A. Samanta, *J. Phys. Chem. B*, 2008, **112**, 16626-16632.
11. T. Iwaki, C. Torigoe, M. Noji and M. Nakanishi, *Biochemistry*, 1993, **32**, 7589-7592.
12. M. A. Haidekker, T. Ling, M. Anglo, H. Y. Stevens, J. A. Frangos and E. A. Theodorakis, *Chem. Biol.*, 2001, **8**, 123-131.
13. M. A. Haidekker and E. A. Theodorakis, *Org. Biomol. Chem.*, 2007, **5**, 1669-1678.
14. C. E. Kung and J. K. Reed, *Biochemistry*, 1986, **25**, 6114-6121.
15. M. K. Kuimova, S. W. Botchway, A. W. Parker, M. Balaz, H. A. Collins, H. L. Anderson, K. Suhling and P. R. Ogilby, *Nat. Chem.*, 2009, **1**, 69-73.
16. F. D. Lewis and X. Zuo, *J. Am. Chem. Soc.*, 2003, **125**, 2046-2047.
17. C. Swalina and M. Maroncelli, *J. Phys. Chem. C*, 2010, **114**, 5602-5610.
18. R. O. Loutfy and B. A. Arnold, *J. Phys. Chem.*, 1982, **86**, 4205-4211.
19. R. O. Loutfy and K. Y. Law, *J. Phys. Chem.*, 1980, **84**, 2803-2808.
20. S. Howell, M. Dakanali, E. Theodorakis and M. Haidekker, *J. Fluoresc.*, 2012, **22**, 457-465.
21. C. Rumble, K. Rich, G. He and M. Maroncelli, *J. Phys. Chem. A*, 2012, **116**, 10786-10792.
22. K. Gavvala, R. K. Koninti, A. Sengupta and P. Hazra, *Phys. Chem. Chem. Phys.*, 2014, **16**, 2823-2826.
23. K. Gavvala, A. Sengupta, R. K. Koninti and P. Hazra, *Phys. Chem. Chem. Phys.*, 2014, **16**, 933-939.

24. K. Gavvala, A. Sengupta, R. K. Koninti and P. Hazra, *J. Phys. Chem. B*, 2013, **117**, 14099-14107.
25. M. J. Frisch, et al. *Gaussian 09*, rev. A.02; Gaussian, Inc.: Wallingford, CT, 2009.
27. N. Díaz, D. Suárez, T. L. Sordo and K. M. Merz, *J. Med. Chem.*, 2001, **44**, 250-260.
28. G. Colmenarejo, *Med. Res. Rev.*, 2003, **23**, 275-301.
29. O. K. Abou-Zied, *RSC Adv.*, 2013, **3**, 8747-8755.
30. P. Bolel, S. Datta, N. Mahapatra and M. Halder, *J. Phys. Chem. B*, 2014, **118**, 26-36.

Table 1. Lifetime, quantum yield, radiative and non-radiative decay rate constants of CCVJ in buffer and in presence of various host molecules.

Sample	a_1[b]	τ_1 (ps)	a_2[c]	τ_2 (ps)	Φ_f[d]	k_r $(ns)^{-1}$	Σk_{nr} $(ns)^{-1}$
CCVJ in buffer	1.00	2.87	-	-	0.0016	0.56	347.87
α-CD 15 mM	0.90	2.90	0.10	16.00	0.0024	0.15	62.35
β-CD 14 mM	0.35	2.90	0.65	35.00	0.02	0.57	28.00
γ-CD 15 mM	0.56	3.00	0.44	24.00	0.0087	0.36	41.30
HSA 100 μM	0.25	3.00	0.75	84.00	0.0895	1.07	10.84

[b] relative amplitude for τ_1; [c] relative amplitude for τ_2 ; [d] ~10% error in measurement.

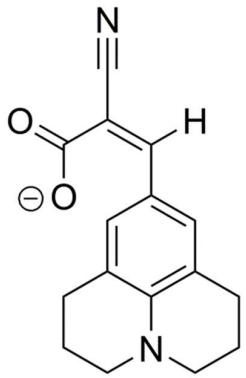

Scheme 1. Chemical structure of CCVJ (E isomer).

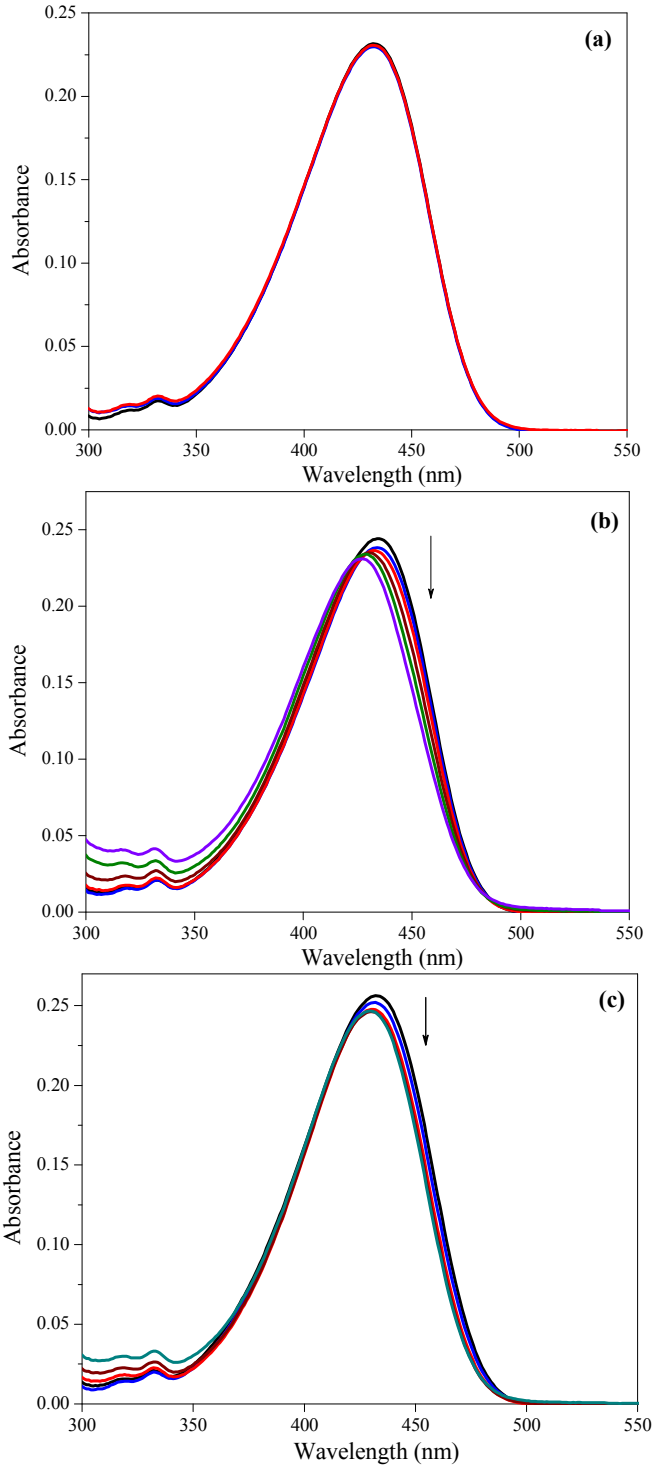

Figure 1. Absorption spectra of CCVJ (10 μM) in presence of (a) α-CD (0 to 10 mM), (b) β-CD (0 to 10 mM) and (c) γ-CD (0 to 10 mM). Arrow indicates the direction of increasing concentration of CD.

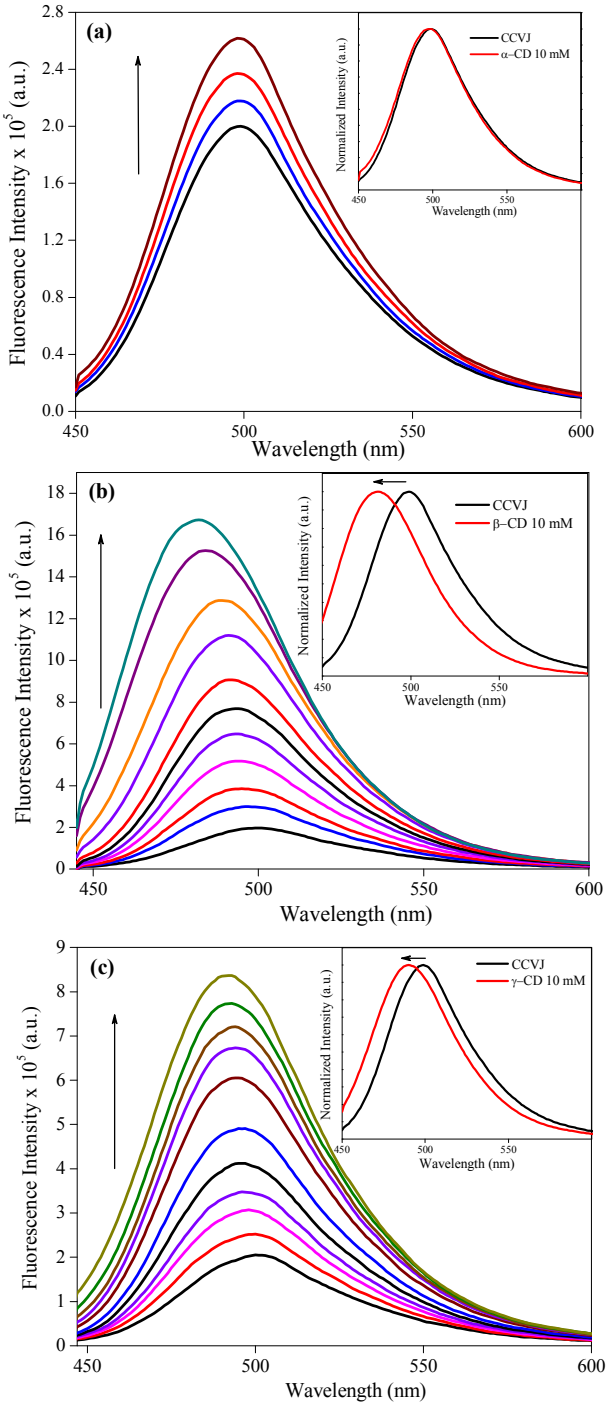

Figure 2. Emission spectra (λ_{ex} = 430 nm) of CCVJ (10 μM) in presence of (a) α-CD (0 to 10 mM), (b) β-CD (0 to 10 mM) and (c) γ-CD (0 to 10 mM). Arrow indicates the direction of increasing concentration of CD.

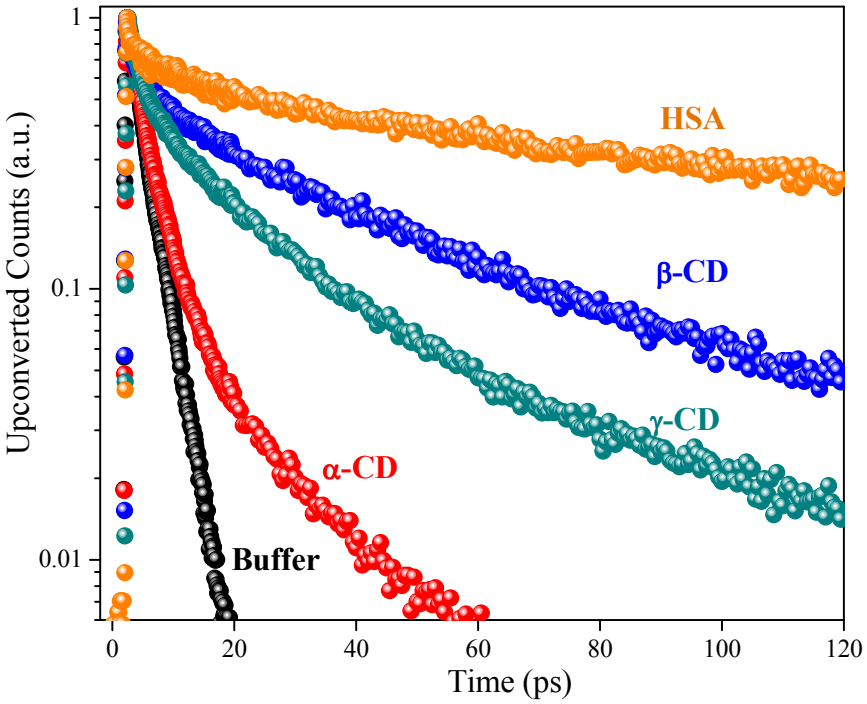

Figure 3. Femtosecond resolved fluorescence decays of CCVJ (~100 μM) in presence of α-CD (15 mM), β-CD (14 mM), γ-CD (15 mM) and HSA (100 μM). Excitation wavelength is 420 nm and collection wavelength is at emission peak maximum.

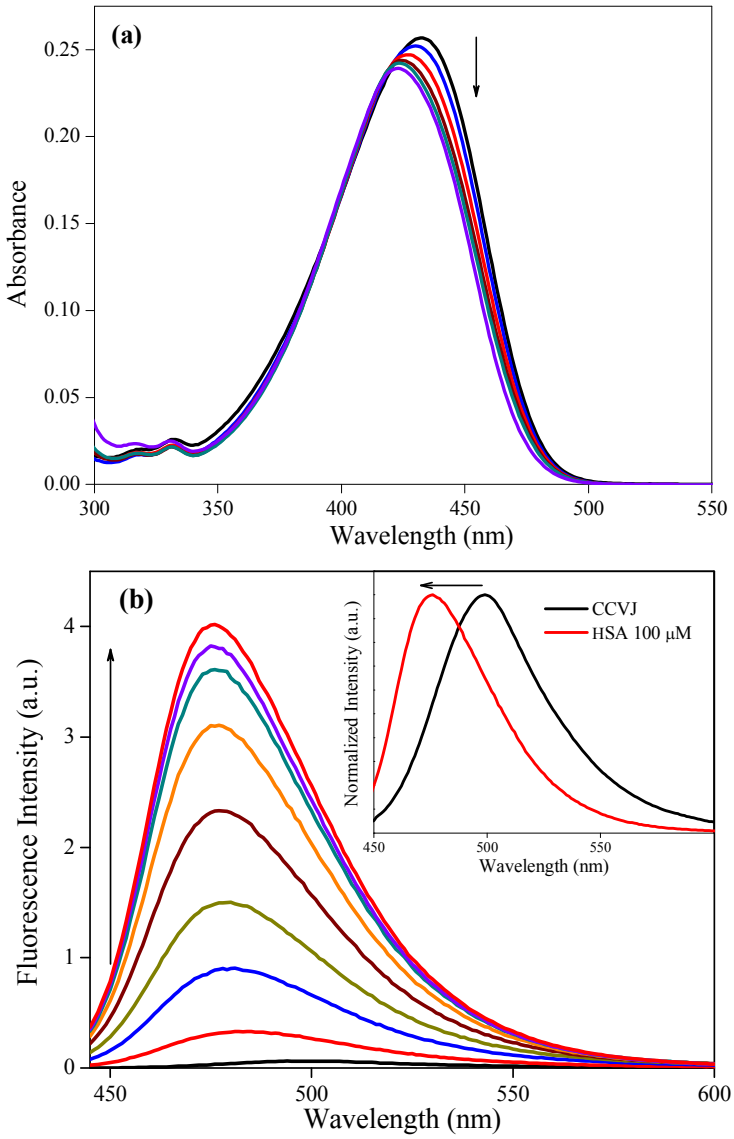

Figure 4. Absorption (a) and emission (b) spectra of CCVJ (10 μM) in presence of HSA (0 to 100 μM). Excitation wavelength is 430 nm. Arrow indicates the direction of increasing concentration of HSA.

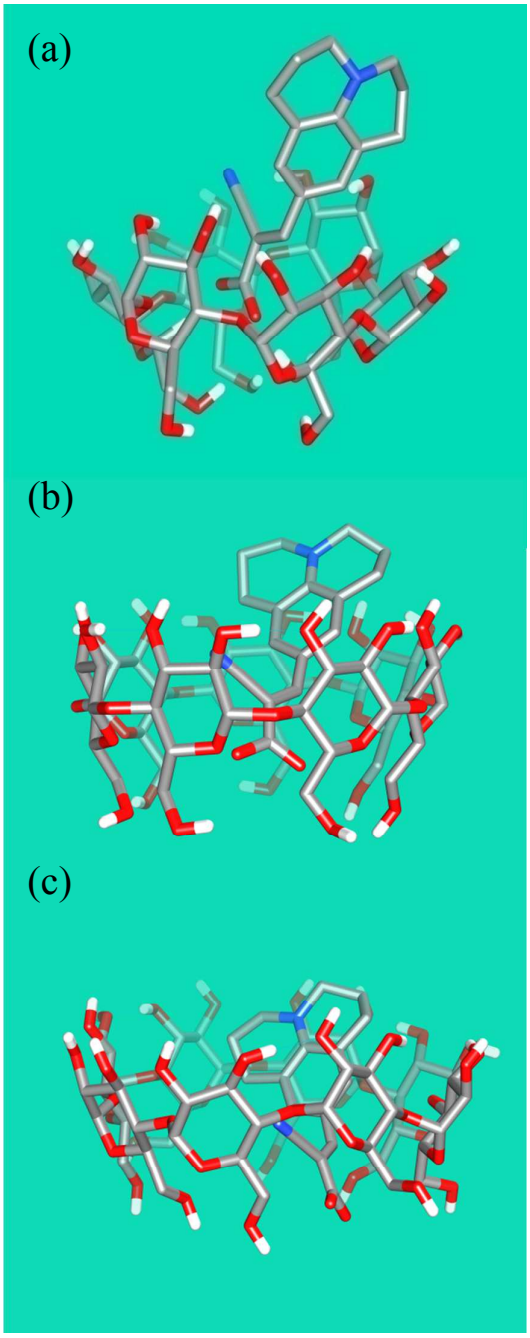

Figure 5. Geometry optimized structures of inclusion complexes of CCVJ with (a) α-CD, (b) β-CD and (c) γ-CD.

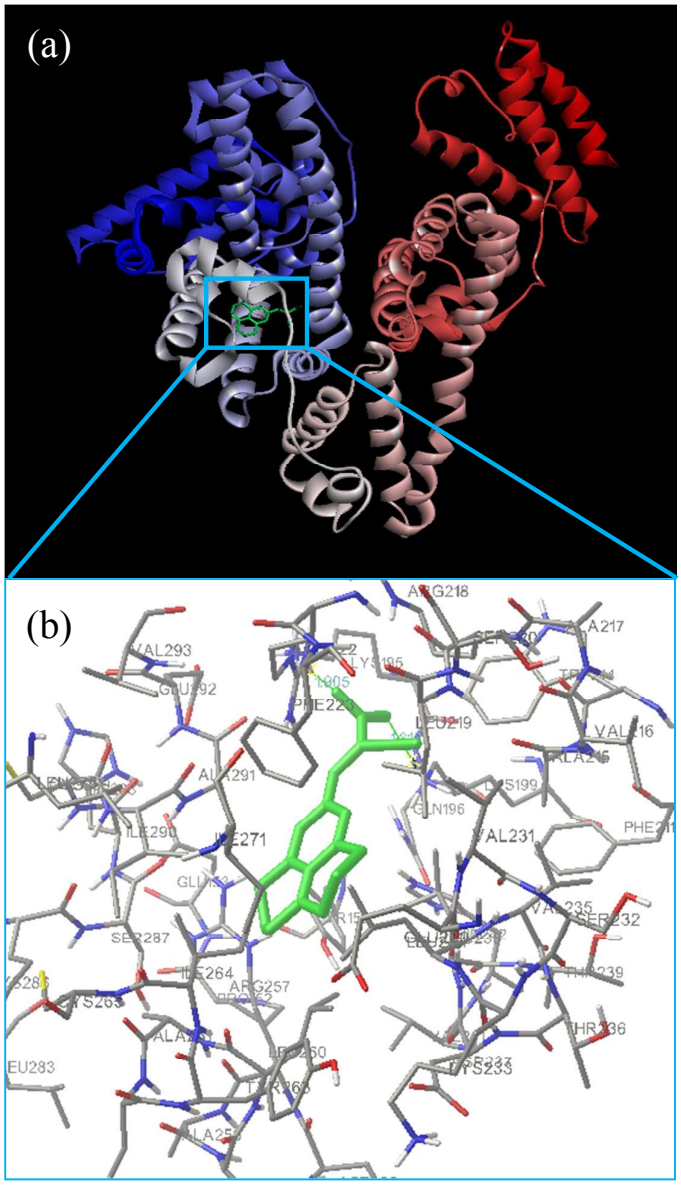

Figure 6. (a) Docked structure of CCVJ complex with HSA. (b) Interaction of CCVJ with amino acids at the binding pocket.

Table of Contents Graphic

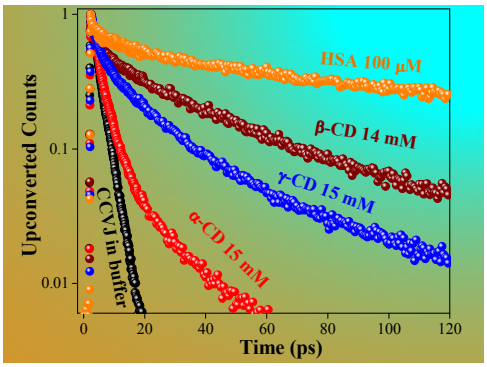

Excited state dynamics of CCVJ are investigated inside the nano-cavities of CD and HSA using steady-state and femtosecond up-conversion techniques.